

# Enhancing the Thermal Stability and Charge Transport Mechanisms in Polyaniline through Holmium Oxide Incorporation for High-Frequency Applications

<sup>1</sup>Anjali Nagaraj Babshetty, <sup>2</sup>Nagbasavanna Sharanappa

<sup>1,2</sup>Department of PG Studies and Research in Physics, Sharnbasva University, Kalaburagi-585103, Karnataka, India

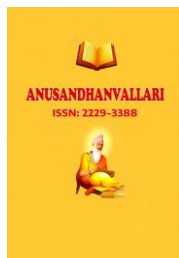
## Abstract

This study presents the synthesis of polyaniline (PANI) and holmium oxide (Ho<sub>2</sub>O<sub>3</sub>) nanocomposites using ammonium dichromate (ADC) as an oxidant through in-situ chemical oxidative polymerization. FESEM analysis confirms a transition from pure PANI's globular morphology to an interconnected network where Ho<sub>2</sub>O<sub>3</sub> nanoparticles are encapsulated. XRD patterns verify the presence of crystalline holmium oxide (20 nm) within the semi-crystalline PANI matrix. FTIR spectroscopy confirms the emeraldine salt state and strong interfacial bonding between PANI amino groups and the Ho<sub>2</sub>O<sub>3</sub> surface. TGA and DSC data reveal enhanced thermal stability, with the composites exhibiting a unique four-step weight loss profile. Electrical characterization shows that both DC and AC conductivity peak at a 25% wt% filler loading. Furthermore, dielectric studies show a high dielectric constant in the MHz range due to Maxwell-Wagner-Sillars interfacial polarization. These findings suggest the material is highly suitable for high-frequency electronics and EMI shielding.

**Keywords:** Polyaniline (PANI), Holmium oxide (Ho<sub>2</sub>O<sub>3</sub>), Ammonium dichromate;(ADC) Nanocomposites, AC/DC conductivity, Thermal stability and Dielectric properties.

## 1. Introduction

The development of multifunctional hybrid nonmaterial's has emerged as a cornerstone of modern materials science, driven by the need for high-performance systems in energy storage, sensing, and electromagnetic interference (EMI) shielding. Among the various classes of materials, conducting polymers (CPs) have garnered significant attention due to their unique electronic and optical properties. Polyaniline (PANI), in particular, stands out as a premier candidate for industrial and scientific applications because of its high electrical conductivity, environmental stability, and ease of synthesis through oxidative polymerization. PANI is characterized by its tunable morphology and its distinct redox chemistry, specifically the transition between its leucoemeraldine, emeraldine, and pernigranite oxidation states. However, pure PANI often faces limitations, such as inferior mechanical stability during repeated redox cycling and moderate power density in electrochemical applications. To overcome these challenges, researchers have turned to the incorporation of inorganic fillers to create PANI-based composites. Rare-earth oxides (REOs) have become increasingly popular as dopants or secondary phases due to their high thermal stability, unique 4f electronic configurations, and paramagnetic properties [1-3]. Holmium oxide (Ho<sub>2</sub>O<sub>3</sub>), a heavy rare-earth sesquioxide, is particularly noteworthy for its high magnetic moment and its ability to exhibit near-infrared (NIR) fluorescence. In electrochemical environments, Ho<sub>2</sub>O<sub>3</sub> has been shown to be electroactive, with redox peaks that can align with those of conducting polymers, thereby facilitating a synergistic effect that enhances the overall capacitance and



stability of the composite. Recent studies indicate that  $\text{Ho}_2\text{O}_3$  nanoparticles can significantly improve the sensitivity of electrochemical sensors and the cycle life of supercapacitor electrodes when integrated into a polymer matrix [3-4].

## 2 Experimental section:

### 2.1: Materials:

Aniline ( $\text{C}_6\text{H}_5\text{NH}_2$ ), Ammonium Dichromate ( $(\text{NH}_4)_2\text{Cr}_2\text{O}_7$ ), Hydrochloric Acid (HCL), and Holmium oxide ( $\text{Ho}_2\text{O}_3$ ), all chemicals were taken S. D. Fine chemicals, During the entire synthesis of PANI and PANI-  $\text{Ho}_2\text{O}_3$  Composites, distilled water has been used.

### 2.2 Synthesis of Pure Polyaniline:

Polyaniline was synthesized via a chemical oxidative polymerization method. Initially, 0.25 M of aniline monomer was dissolved in 1 N HCl under constant magnetic stirring to facilitate the formation of aniline hydrochloride. To initiate the polymerization, a 0.25 M aqueous solution of Ammonium Dichromate (ADC) was added dropwise to the mixture. The reaction was maintained at ambient temperature for 5 hours with continuous stirring to ensure complete polymerization. Post-reaction, the resulting mixture was left undisturbed overnight to allow the polymer precipitate to settle. The sample was subsequently collected through vacuum filtration and washed repeatedly with distilled water and 1 N HCl to remove any unreacted monomers and oxidant residues. Finally, the obtained product was dried in an oven to remove residual moisture and then ground into a fine, uniform powder to obtain pure polyaniline in its emeraldine salt form.

### 2.3 Synthesis of PANI- $\text{Ho}_2\text{O}_3$ Nanocomposites

The PANI-  $\text{Ho}_2\text{O}_3$  nanocomposites were synthesized via a facile in-situ chemical oxidative polymerization technique. The procedure followed the same experimental parameters as the synthesis of pure polyaniline, with the strategic addition of the inorganic phase. Specifically, stoichiometric amounts of holmium oxide ( $\text{Ho}_2\text{O}_3$ ) were dispersed into the aniline-HCl solution prior to the initiation of polymerization. To investigate the effect of filler concentration, composites were prepared with varying weight percentages (wt %) of  $\text{Ho}_2\text{O}_3$ . The mixture was subjected to vigorous magnetic stirring for 5 hours at ambient temperature to ensure a uniform distribution of the nanoparticles within the growing polymer matrix. Upon completion of the reaction, the composite precipitate was allowed to settle overnight. The resulting product was purified using vacuum filtration and washed repeatedly with distilled water and 1 N HCl to eliminate unreacted species and impurities. The obtained nanocomposites were dried thoroughly and ground into a fine powder for subsequent characterization.

## 3. Results and Discussion:

### 3.1 TGA Analysis:

#### 3.1.1 Pure PANI

The Thermogravimetric Analysis (TGA) of pure polyaniline (PANI) typically exhibits a characteristic four-step weight loss pattern, which is evident in the below figure 1. First-step is due to moisture and solvent evaporation in the range of up to  $\sim 120^\circ\text{C}$ , the loss of physically adsorbed water and any residual volatile solvents trapped in the polymer matrix. Second –step is in the range of  $\sim 150^\circ\text{C}$ – $350^\circ\text{C}$  is due to De-doping and Dopant loss, this corresponds to the elimination of the dopant molecules and the evolution of small volatile fragments. The slope suggests a gradual de-doping process. Third step is due to the initial backbone degradation in the temperature range of  $\sim 400^\circ\text{C}$ – $600^\circ\text{C}$ , there is a visible change in the graph around  $500^\circ\text{C}$  this represents the beginning of

the structural breakdown of the polyaniline backbone, specifically the scission of the C-N-C bonds and the degradation of the benzenoid and quinonoid rings. The PANI remains relatively stable up to 400 °C before the major backbone collapse occurs, which is a good indicator of high-quality polymerization using ADC[6-8]. The last step weight loss is due to major carbonization and char formation in the temperature range between 700 °C - 900 °C this is the final stage of thermal decomposition where the remaining organic structure carbonizes, leaving behind a carbonaceous residue. In PANI synthesized with ADC, the residue is higher[5-7].

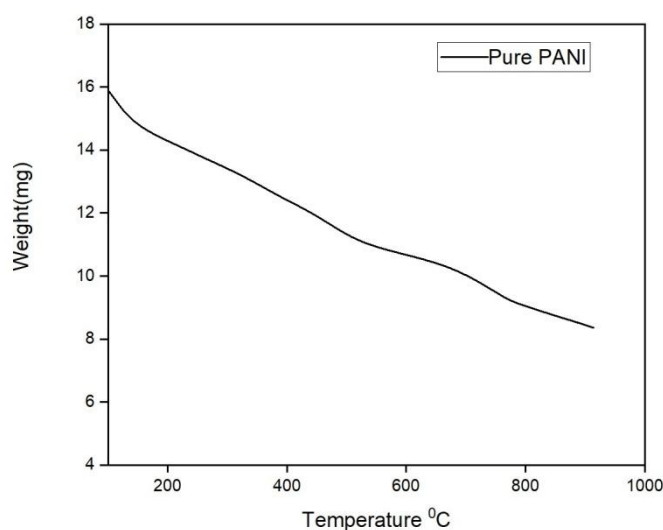
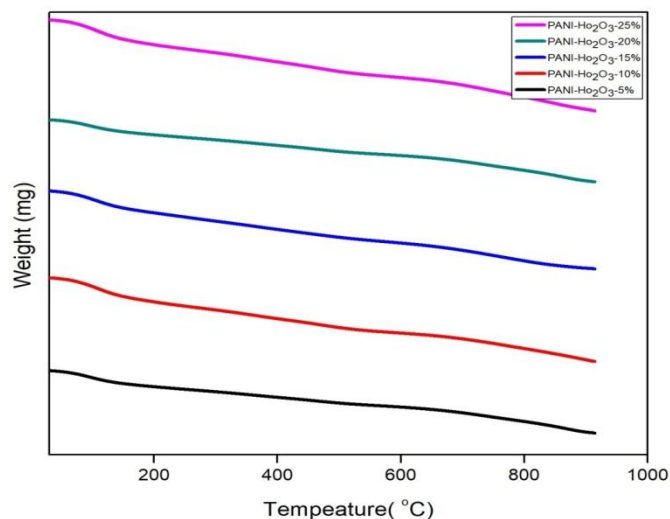


Figure 1: TGA plot of Pure PANI

### 3.1.2. TGA Analysis of PANI-HO<sub>2</sub>O<sub>3</sub> Composites:

Holmium oxide and polyaniline composite will exhibit a four-step weight loss in its TGA analysis with all of five different weight percentages of Ho<sub>2</sub>O<sub>3</sub> (5%, 10%, 15%, 20% & 25%) illustrating in below figure 2. Holmium oxide is rare earth oxide is generally thermally stable at the temperature where polyaniline degrades. Their incorporation into the polyaniline matrix often leads to enhanced thermal stability of the composites. First weight loss in the temperature range is 50°C-180°C is because of evaporation of loosely bound volatile impurities and moisture. Second weight loss is due to loss of dopant and potentially any residual strongly bound synthesized solvents in the temperature range of 181°C-340°C, third weight loss is from 350°C-550°C is due to initial degradation of the PANI backbone, possibly involving scission of weaker bonds or decomposition of certain segments. Last step weight loss is from 551°C-790°C major thermal decomposition and carbonization of the main polyaniline chains. Ho<sub>2</sub>O<sub>3</sub> is enhancing the thermal stability, shifting this step to higher temperature or reducing its rate[8].

The primary reason for improved thermal stability in polyaniline-rare earth oxide composites is due to high thermal stability of rare earth oxides and have very high melting points (above 2000 °C) and are thermally stable in the temperature range where polyaniline degrades. Interfacial interactions between the hydroxyl groups on the surface of the rare earth oxide nanoparticles and the imine/amine groups of the polyaniline chain can restrict the segmental motion of the polymer chains. This increased rigidity can lead to higher thermal stability. Ho<sub>2</sub>O<sub>3</sub> doped polyanilines are expected to be more thermally stable compared to pure polyaniline[9].



**Figure 2: TGA graph of PANI-Ho<sub>2</sub>O<sub>3</sub> Composites**

### 3.2. Differential scanning calorimetry (DSC):

#### 3.2.1 Pure PANI:

The interpretation of the differential scanning calorimetry analysis of pure PANI is as shown in the figure 3. DSC is powerful thermal analysis technique used to study the heat flow associated with phase transition and chemical reaction in materials as a function of temperature. The graph shows a distinct endothermic peak around 111.2<sup>o</sup> C, this is primarily attributed to the evaporation of physically adsorbed water and potentially residual solvent trapped within the polymer matrix. This broad endothermic region typically represents a combination of thermal de-doping and the onset of the structural breakdown of the PANI backbone. PANI is often amorphous, thermal treatment can induce changes in its crystallinity

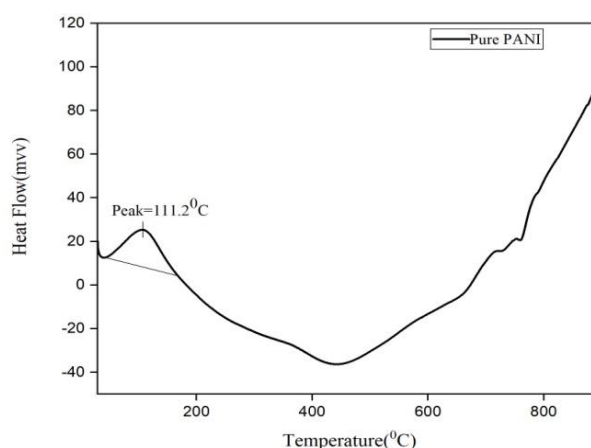


**Figure 3: DSC thermograms of Pure PANI**

#### 3.2.2: Polyaniline- holmium oxide composites

The thermal behavior of Polyaniline(PANI) composites with increasing weight percentages(5%, 10%, 15%, 20%, and 25%) of Holmium oxide(Ho<sub>2</sub>O<sub>3</sub>), we look at how the dopant concentration shifts the characteristic peaks on a DSC curve as shown in figure 4 the graph shows a broad endothermic peaks at 78.2<sup>o</sup>C this is due to a

classic signature for the evaporation of volatile components, primarily adsorbed moisture polyaniline is hydrophilic, and  $\text{Ho}_2\text{O}_3$  often increases the surface area or changes the porosity, leading to significant moisture retention. As at the low concentration (5%, 10%, and 15%) the PANI matrix is dominant. The thermal degradation occurs earlier because of the loss of moisture. As the concentration level increases from (20% and 25%) the  $\text{Ho}_2\text{O}_3$  particles provide better thermal shielding. The onset of backbone decomposition is often delayed to higher temperature compared to the low doping composites. This broad endothermic peak is attributed to the dehydration process and at 25% loading of  $\text{Ho}_2\text{O}_3$ , the metal oxide particles likely create a high surface area that retains moisture the slope of the curve beyond  $120^\circ\text{C}$  is relatively steady this suggests that the  $\text{Ho}_2\text{O}_3$  particles are effectively integrated, providing a degree of thermal shielding of the PANI backbone. At high concentrations usually increase the overall thermal conductivity of the sample compared to pure PANI[10-11].

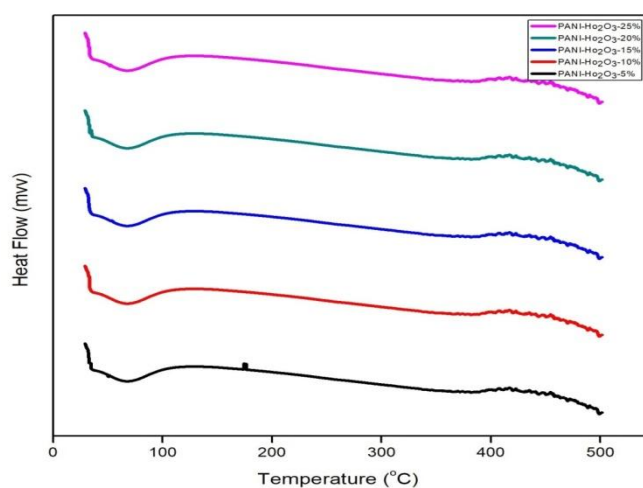


Figure 4: DSC Thermograms of PANI-  $\text{Ho}_2\text{O}_3$  Composites

### 3.3.Xray Diffraction:

#### 3.3.1: Pure PANI:

The X-ray diffraction pattern of the pure PANI synthesized using ammonium dichromate (ADC) as an oxidant, as shown in the below figure 5, pure polyaniline exhibits characteristics typical of a semi-crystalline conducting polymer. The diffractogram shows a broad, humped peak centered between  $2\theta \approx 20^\circ$  and  $25^\circ$  this feature is a hallmark of the amorphous nature of PANI. The broad peak centered at approximately  $2\theta \approx 25^\circ$  corresponds to the  $\pi - \pi$  stacking or the characteristic distance between the aromatic rings in adjacent polymer chains it represents the (020) crystallographic plane. During synthesis, the dichromate ions or their reduced chromium by-products can sometimes act as counter-ions, slightly shifting the diffraction peaks compared to PANI synthesized with other oxidants.

The crystallite size (D) can be estimated from the broadening of the XRD peaks using the Debye-Scherrer's equation:

$$D = \frac{K\lambda}{\beta \cos\theta}$$

Where D = average crystallite size

K = shape factor (nearly 0.9)

$\lambda$  = X-ray wavelength (for Cu Ka radiation,  $\lambda = 1.5406\text{\AA}$ )

$\beta$  = Full width at half maximum (FWHM) of the diffraction peak in radians =  $2.5^\circ$

$\theta$  = Bragg angle (half of the  $2\theta$  value)

The average crystallite size is  $D \approx 3.26\text{nm}$ , pure PANI graph as shown in figure 5 shows a very low intensity and a very broad peak. This suggests that PANI has very low crystallinity because of using ammonium dichromate as an oxidant often lead to a more disordered polymer chain. Because the crystallites are so small, the material will be behaving differently than standard bulk PANI, resulting in a massive surface-to-volume ratio. This makes PANI a highly reactive material and this leads to lower overall conductivity compared to PANI with larger crystallites, because the disordered boundaries act as speed bumps for electricity. Since PANI exhibits a small crystallite size of  $3.26\text{nm}$ , it's possible for the material to transition from a conductor to a dielectric.

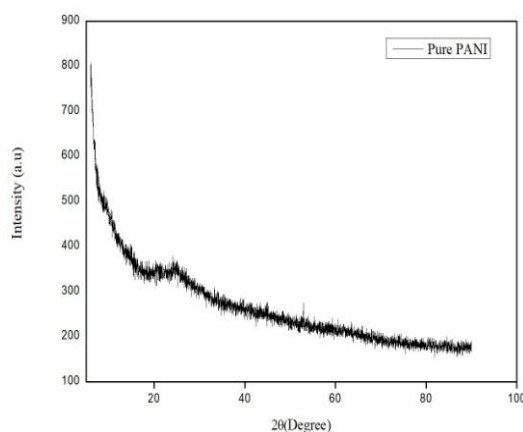


Figure 5: XRD Pattern of Pure PANI

### 3.3.2: Polyaniline-Holmium Oxide Composites:

The X-ray diffraction (XRD) patterns for your PANI- $\text{Ho}_2\text{O}_3$  nanocomposites (5%, 10%, 15%, 20%, and 25%) synthesized with Ammonium Dichromate (ADC) reveal the structural interaction between the amorphous polymer matrix and the crystalline rare-earth oxide dopant as shown below figure 6. All Composites exhibit a broad hump centered around  $2\theta \approx 20^\circ$  to  $25^\circ$ . This characteristic broad peak is attributed to the periodically parallel and perpendicular stacking of the polyaniline chains, confirming the semi-crystalline nature of the PANI matrix. Superimposed on the broad PANI base, there are sharp, narrow diffraction peaks, most notably the distinct peak appearing near  $2\theta \approx 33^\circ$ . These sharp peaks correspond to the cubic phase of Holmium Oxide ( $\text{Ho}_2\text{O}_3$ ). As the weight percentage (wt %) of  $\text{Ho}_2\text{O}_3$  increases from 5% to 25%, the intensity of the crystalline peaks associated with the rare-earth oxide becomes more prominent. The stability of the peak positions suggests that the  $\text{Ho}_2\text{O}_3$  nanoparticles maintain their crystalline integrity and are successfully embedded within the polymer matrix without undergoing chemical phase changes during the in-situ polymerization process. The presence of these peaks confirms the formation of a true nanocomposite. The crystallite size ( $D$ ) can be estimated from the broadening of the XRD peaks using the Debye-Scherrer's equation:

$$D = \frac{K\lambda}{\beta \cos\theta} = 20\text{nm}$$

As a result, the transition from pure PANI to the PANI- $\text{Ho}_2\text{O}_3$  composites represents a significant shift in the size from  $3.23\text{nm}$  to  $20\text{nm}$  crystallite size. The crystallite size of holmium oxide is particularly beneficial for dielectric applications because the particles are relatively large compared to the  $3.23\text{nm}$  PANI domains; they

provide a significant surface area for charge accumulation, which boosts the overall capacitance of the material[11-12].

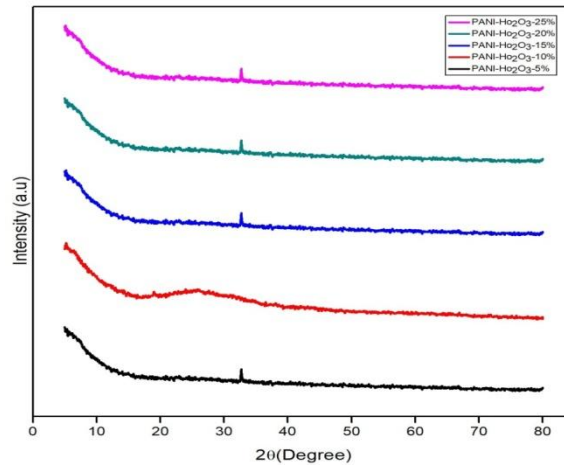


Figure 6: XRD patterns of PANI-H<sub>2</sub>O<sub>3</sub> composites

### 3.4. FESEM Analysis:

#### 3.4.1: Pure PANI:

The FESEM (Field Emission scanning Electron Microscopy) analysis of pure polyaniline image is as shown below figure 7. PANI is a crucial technique used to determine its surface morphology, particles size, and structural features, all of which heavily influence the polymer's properties. The morphology of pure PANI is highly dependent on the synthesis conditions PANI shows a granular or particulate using ADC, the PANI often exhibits a structure composed of irregularly composed granules and flakes. Regardless of the macroscopic PANI often exhibits the high surface area and porosity, which determines its suitability for various advanced application like sensors, super capacitors

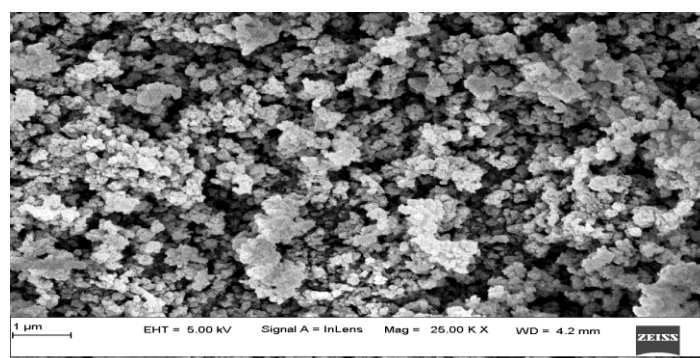


Figure 7: FESEM image of Pure PANI

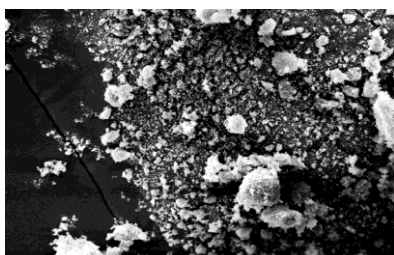
### 3.4.2 Polyaniline-Holmium Oxide (PANI-Ho<sub>2</sub>O<sub>3</sub>) composites

The interface between the holmium oxide (Ho<sub>2</sub>O<sub>3</sub>) and the PANI matrix composite structural morphology is done by FESEM analysis of PANI-Ho<sub>2</sub>O<sub>3</sub> composites provide critical evidence of the composite's morphological evolution and elemental increases from 5%, 10%, 15%, 20% and 25%. The analysis confirms the successful incorporation of the rare-earth oxide and explains the property changes seen at different weight percentage the FESEM images of PANI-Ho<sub>2</sub>O<sub>3</sub> composites shown in below figure 8. At low concentration (PANI-Ho<sub>2</sub>O<sub>3</sub>-5% and PANI-Ho<sub>2</sub>O<sub>3</sub>-10%), the Ho<sub>2</sub>O<sub>3</sub> particles act as isolated nucleation centers, which can lead to a relatively uniform PANI matrix with small, bright dots widely dispersed the uniform coating maximizes the interfacial area between the PANI and Ho<sub>2</sub>O<sub>3</sub>, leading to optimal coupling and enhanced composite properties.

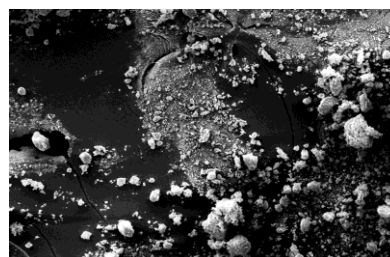
At intermediate concentration, PANI-Ho<sub>2</sub>O<sub>3</sub>-15%, the distance between the rare-earth particles decreases and the bright regions (holmium) begin to appear closer together. The PANI grains start to form bridges between the Ho<sub>2</sub>O<sub>3</sub> clusters, creating a continuous conductive path that is highly beneficial for electrical properties.

At high concentration (PANI-Ho<sub>2</sub>O<sub>3</sub>-20% and PANI-Ho<sub>2</sub>O<sub>3</sub>-25%), the morphology typically shifts toward agglomeration. The composites become much busier with large brighter crystalline masses. Due to the high surface energy Ho<sub>2</sub>O<sub>3</sub> nanoparticles the PANI prefers to grow on these particles, leading to the decorated appearance where the polymer layer wrap around the oxide core. The fast polymerization with ADC often leads to a higher degree of amorphous regions compared to crystalline ones [13-14].

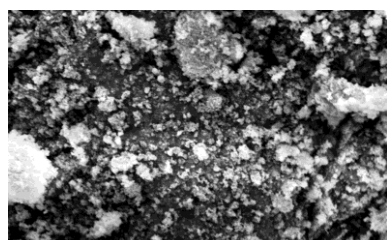
a) PANI-Ho<sub>2</sub>O<sub>3</sub>-5%



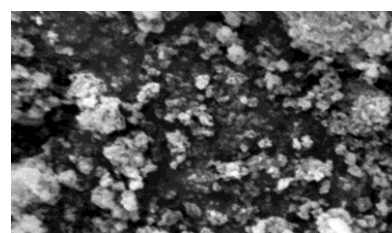
b) PANI-Ho<sub>2</sub>O<sub>3</sub>-10%



c) PANI-Ho<sub>2</sub>O<sub>3</sub>-15%



d) PANI-Ho<sub>2</sub>O<sub>3</sub>-20%



e) PANI-Ho<sub>2</sub>O<sub>3</sub>-25%

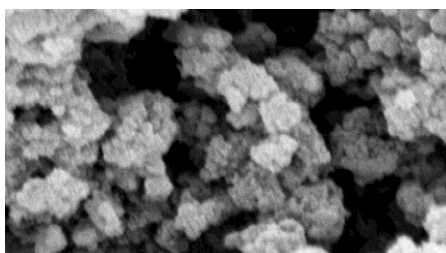


Figure 8: FESEM images of PANI- Ho<sub>2</sub>O<sub>3</sub> composites

### 3.5 FTIR Analysis

#### 3.5.1 Pure PANI

The Fourier Transform Infrared (FTIR) spectrum of pure polyaniline (PANI) shown in figure 9 displays the characteristic vibrational bands that confirm its chemical structure and conducting state. The spectrum exhibits several key absorption bands associated with the emeraldine salt form of PANI:

- 3063  $\text{cm}^{-1}$ : This broad band is attributed to the N-H stretching vibrations of the amine groups.
- 1578  $\text{cm}^{-1}$ : This peak corresponds to the C=C stretching vibration of the quinonoid (Q) ring, which is a hallmark of the oxidized state of PANI.
- 1500  $\text{cm}^{-1}$ : This band is assigned to the C=C stretching vibration of the benzenoid (B) ring, representing the reduced units in the polymer chain.
- 1312  $\text{cm}^{-1}$  and 1341  $\text{cm}^{-1}$ : These peaks are associated with C-N stretching vibrations of the secondary aromatic amines.
- 1253  $\text{cm}^{-1}$ : This band relates to the C-N stretching of the benzenoid unit.
- 1150  $\text{cm}^{-1}$ : Often referred to as the electronic-like band, this vibration is associated with the vibration of the dopant and the delocalization of electrons, indicating high electrical conductivity.
- 826  $\text{cm}^{-1}$ : This peak represents the C-H out-of-plane bending vibration of the para-disubstituted benzene rings, confirming the linear polymerization of aniline.
- 694  $\text{cm}^{-1}$ : This is typically associated with the out-of-plane C-H bending or ring deformation.

The broadness of vibrational bands and the prominent N-H stretching region indicate a highly disordered, amorphous dominant structure, which limits long range electronic delocalization despite the presence of dopant related peaks.

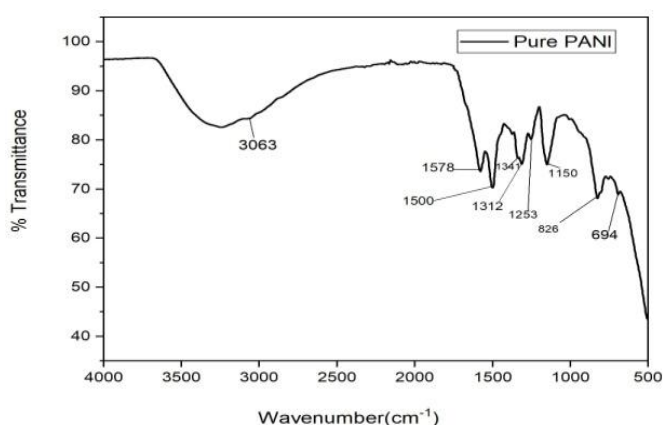
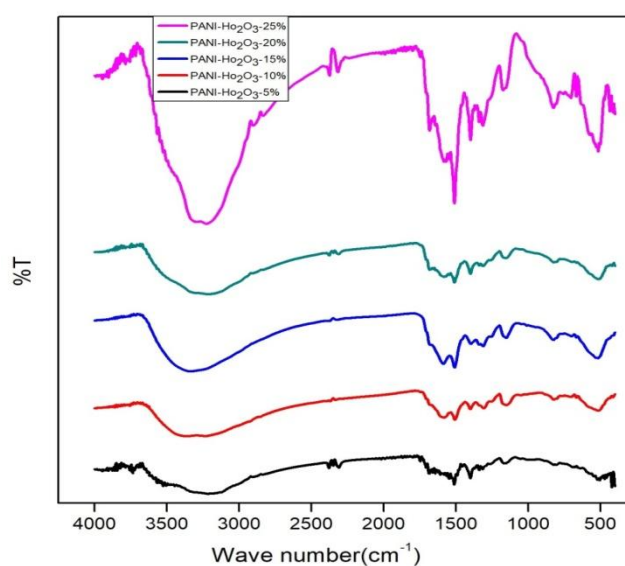


Figure 9: FTIR spectra of Pure PANI

#### 3.5.2 Polyaniline-Holmium Oxide Composites

The FTIR spectra for the PANI-Ho<sub>2</sub>O<sub>3</sub> composites (5%, 10%, 15%, 20%, and 25% loading) synthesized with Ammonium Dichromate (ADC) show the introduction of the rare-earth oxide influences the chemical environment of the polyaniline matrix the FTIR spectra of PANI-Ho<sub>2</sub>O<sub>3</sub> composites are shown in figure 10. Preservation of PANI Backbone: All composite samples retain the characteristic peaks of polyaniline,

specifically the quinonoid (Q) and benzenoid (B) ring stretching vibrations in the  $1500\text{ cm}^{-1}$  and  $1600\text{ cm}^{-1}$  region. This confirms that the in-situ polymerization successfully formed the PANI matrix around the  $\text{Ho}_2\text{O}_3$  nanoparticles without disrupting the polymer's primary structure. **Broadening of N-H Band:** As concentration of  $\text{Ho}_2\text{O}_3$  increases from 5% to 25%, strengthening of the interfacial interaction between the  $\text{Ho}^{3+}$  ions and the PANI nitrogen atoms. At 25% of PANI- $\text{Ho}_2\text{O}_3$  Composite, the peaks become exceptionally sharp and intense. This suggests that  $\text{Ho}_2\text{O}_3$  acts as a structural template, enhancing the molecular ordering and crystallinity of the PANI chains. The broad absorption band in the  $3000\text{ cm}^{-1}$  -  $3500\text{ cm}^{-1}$  region, associated with N-H stretching, appears more pronounced or shifted in the composites compared to pure PANI. This is likely due to hydrogen bonding interactions between the PANI amino groups and the oxygen atoms on the surface of the  $\text{Ho}_2\text{O}_3$  particles. This strongest evidence of chemical interaction between the organic and inorganic phases. **Metal-Oxygen (M-O) Vibrations:** In the lower wavenumber region  $400\text{ cm}^{-1}$  -  $600\text{ cm}^{-1}$ , new or intensified vibrational modes are visible, which are characteristic of the Ho-O stretching vibrations. As the weight percentage (wt%) of  $\text{Ho}_2\text{O}_3$  increases from 5% to 25%, the intensity of the peaks associated with the inorganic phase becomes more distinct, while some PANI-specific bands may show slight shifts toward lower wavenumbers. These shifts indicate a strong interfacial interaction between the polymer chains and the nanoparticles[15-17].



**Figure 10: FTIR Spectra of PANI-  $\text{Ho}_2\text{O}_3$  Composite**

### 3.6. Electrical Properties

#### 3.6.1 AC Conductivity: Pure PANI and PANI- $\text{Ho}_2\text{O}_3$ Composite

The analysis of the AC conductivity ( $\sigma_{ac}$ ) for Pure PANI and its Holmium Oxide  $\text{Ho}_2\text{O}_3$  doped nanocomposites (5% to 25% wt), synthesized using Ammonium Dichromate (ADC) as the oxidant, as shown in figure 11. All composites exhibit conductivity that varies with frequency, confirming that charge transport occurs via a hopping mechanism (likely Correlated Barrier Hopping or Variable Range Hopping). Distinct peaks are visible across all composites, particularly a prominent peak near 3MHz to 4MHz. These indicate molecular relaxation processes or resonance where the hopping frequency of the charge carriers matches the frequency of the applied AC field. Pure PANI (the bottom black curve) shows baseline conductivity characteristic of the emeraldine salt phase achieved via ammonium dichromate oxidation. As the weight percentage of  $\text{Ho}_2\text{O}_3$  increases (from 5% to 25%), the overall magnitude of the AC conductivity shifts upward. This demonstrates that the rare-earth oxide nanoparticles act as conductive bridges or increase the density of localized states, facilitating more efficient

charge transport through the polymer matrix. The increase in conductivity with higher filler loading is largely due to the accumulation of charges at the interfaces between the amorphous PANI and the crystalline  $\text{Ho}_2\text{O}_3$  nanoparticles due to interfacial Polymerization (MWS Effect). At the PANI- $\text{Ho}_2\text{O}_3$ -25% loading, the composite reaches its optimal electrical performance, suggesting a well-developed interconnected network that minimizes the barrier for polaron hopping. The AC conductivity for Pure PANI and  $\text{Ho}_2\text{O}_3$  doped PANI (5–25% wt) show a strong dependence on both frequency and dopant concentration. The synthesis using ADC oxidant results in a highly conjugated system where the addition of  $\text{Ho}_2\text{O}_3$  systematically increases conductivity. The presence of relaxation peaks in the MHz range suggests significant interfacial polarization, with the 25% loading showing the maximum response, making these materials ideal for high-frequency electronic applications.

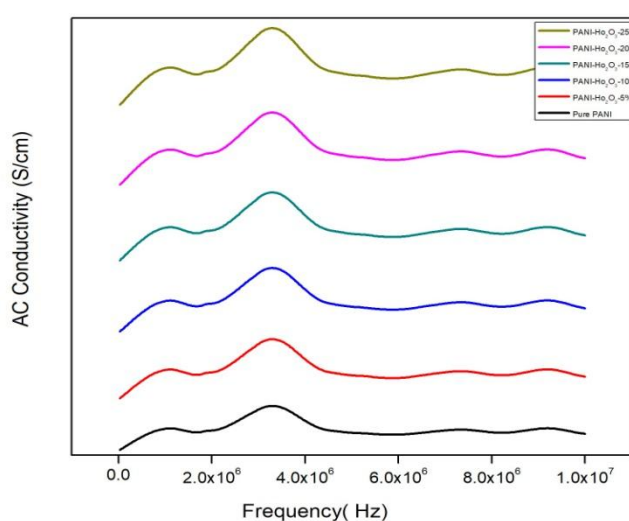


**Figure 11: AC Conductivity Curves of Pure PANI and PANI-  $\text{Ho}_2\text{O}_3$  Composites**

### 3.6.2. DC Conductivity: Pure PANI and PANI- $\text{Ho}_2\text{O}_3$ Composites

The analysis of the DC conductivity ( $\sigma_{dc}$ ) for Pure PANI and holmium oxide ( $\text{Ho}_2\text{O}_3$ ) doped PANI nanocomposites, synthesized with ammonium dichromate (ADC) as an oxidant, temperature-dependent graph is as shown in figure 12. For all Composites, including pure PANI, the conductivity initially decreases slightly as the temperature rises from room temperature to approximately  $100^\circ\text{C}$ . Beyond this point, the conductivity stabilizes and becomes nearly independent of temperature up to  $200^\circ\text{C}$ . This behavior suggests good thermal stability of the electrical properties in this temperature range. There is a significant and systematic increase in DC conductivity with the increasing weight percentage (wt%) of holmium oxide. Pure PANI Exhibits the lowest baseline conductivity (bottom black curve). As doping concentration increases from 5% to 25%, the curves shift upward. The 25% of PANI-  $\text{Ho}_2\text{O}_3$  composite displays the highest conductivity across the entire temperature spectrum. The improvement in conductivity with doping suggests that the rare-earth oxide nanoparticles facilitate charge transport. This is likely achieved by providing more hopping sites or improving the connectivity between PANI chains, lowering the activation energy required for charge carriers (polarons) to move through the matrix. The use of ammonium dichromate as an oxidant produces a highly conjugated polyaniline backbone in its conductive emeraldine salt phase. The stability observed at elevated temperatures confirms the robustness of the polymer synthesized with this specific oxidant. The DC conductivity of pure PANI and PANI- $\text{Ho}_2\text{O}_3$  composites was evaluated as a function of temperature ( $30^\circ\text{C}$  to  $200^\circ\text{C}$ ). The results demonstrate that conductivity increases systematically with  $\text{Ho}_2\text{O}_3$  content. The stability of the conductivity at higher temperatures highlights the effectiveness of ADC as an oxidant and the synergistic interaction between

the conductive PANI matrix and the  $\text{Ho}_2\text{O}_3$  dopants, making these materials suitable for temperature-stable electronic applications.

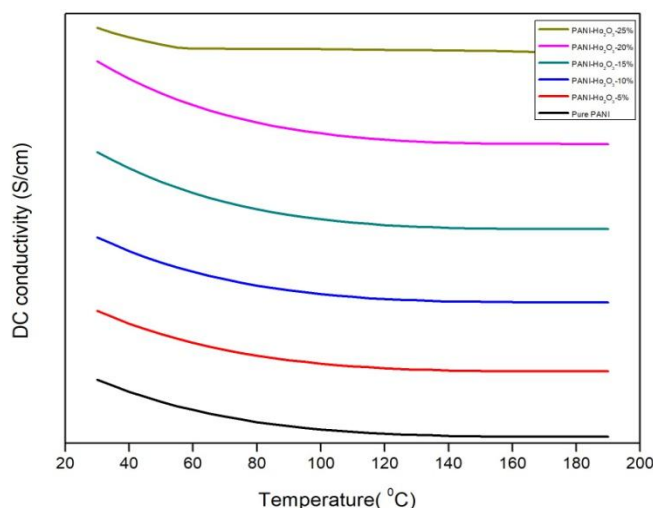


**Figure 12: DC conductivity of Pure PANI and PANI-  $\text{Ho}_2\text{O}_3$  Composites**

### 3.6.3. Dielectric Constant: Pure PANI and PANI- $\text{Ho}_2\text{O}_3$ Composites

The dielectric constant ( $\epsilon'$ ) analysis for Pure PANI and its holmium oxide ( $\text{Ho}_2\text{O}_3$ ) doped nanocomposites (5%, 10%, 15%, 20%, and 25%), synthesized using ammonium dichromate (ADC) as an oxidant, reveals the material stores electrical energy under an applied field as shown in figure 13. The dielectric constant remains remarkably stable across a broad frequency range, from 0 to 8 MHz. This stability is crucial for electronic applications requiring consistent performance over a wide bandwidth. A sharp, exponential-like increase in the dielectric constant is observed as the frequency approaches  $1.0 \times 10^{-7}$  Hz. This behavior suggests a resonance effect or the onset of rapid polarization transitions at very high frequencies. There is a clear, systematic increase in the dielectric constant as the weight percentage (wt%) of  $\text{Ho}_2\text{O}_3$  increases from 5% to 25%. Pure PANI (bottom curve) shows the lowest dielectric constant, while the 25%  $\text{Ho}_2\text{O}_3$  composite (top curve) exhibits the highest values. The increase in dielectric constant with higher filler is attributed to Maxwell-Wagner-Sillars (MWS) polarization. The presence of  $\text{Ho}_2\text{O}_3$  nanoparticles creates a high density of interfaces between the crystalline nanoparticles and the amorphous PANI matrix, where charge carriers (polarons) accumulate, leading to enhanced polarization. The frequency-dependent dielectric constant of Pure PANI and PANI- $\text{Ho}_2\text{O}_3$  nanocomposites was investigated. The stability of the dielectric constant at low-to-mid frequencies followed by a sharp increase in the MHz range indicates robust interfacial polarization at the polymer-nanoparticle junctions. The integration of  $\text{Ho}_2\text{O}_3$  into PANI synthesized with ADC oxidant effectively optimizes the material's energy storage capabilities for high-performance capacitor applications.

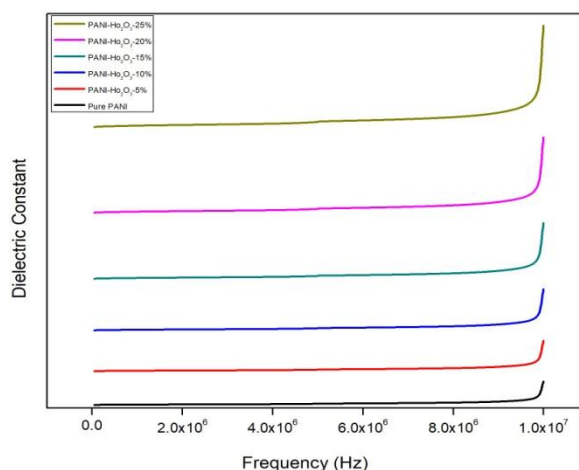


**Figure 13: Dielectric Constant of Pure PANI and PANI-Ho<sub>2</sub>O<sub>3</sub> Composites**

### 3.6.3. Dielectric loss: Pure PANI and PANI-Ho<sub>2</sub>O<sub>3</sub> Composites

The dielectric loss ( $\epsilon''$ ) behavior for Pure PANI and holmium oxide Ho<sub>2</sub>O<sub>3</sub> doped PANI nanocomposites (5% to 25% wt), synthesized with ammonium dichromate (ADC) as the oxidant, show energy dissipation changes with frequency and filler concentration as shown in figure 14. All Composites, including Pure PANI, show high dielectric loss at lower frequencies that drops sharply as frequency increases. This is primarily due to space charge polarization and the contribution of DC conductivity to the overall loss. At low frequencies, charge carriers have enough time to accumulate at the grain boundaries between the conductive PANI and the Ho<sub>2</sub>O<sub>3</sub> nanoparticles. As the frequency moves toward the MHz range the dielectric loss curves flatten out and become nearly independent of frequency. This stable behavior is advantageous for high-frequency electronic applications where constant dissipation properties are required to prevent overheating. There is a clear systematic increase in dielectric loss as the weight percentage of holmium oxide increases. The 25% Ho<sub>2</sub>O<sub>3</sub> composite (top curve) exhibits the highest dielectric loss. This correlates with the higher AC conductivity observed in these composites more charge carriers and hopping sites lead to greater energy dissipation through conduction and polarization lag. The frequency-dependent dielectric loss of Pure PANI and Ho<sub>2</sub>O<sub>3</sub> -doped PANI nanocomposites was studied. The results show that dielectric loss decreases rapidly at low frequencies due to space charge effects and stabilizes in the high-frequency regime. The systematic enhancement of dielectric loss with increasing Ho<sub>2</sub>O<sub>3</sub> content (up to 25% wt%) confirms a higher degree of interfacial polarization and electronic transport within the composite matrix synthesized with ADC oxidant[17-20].

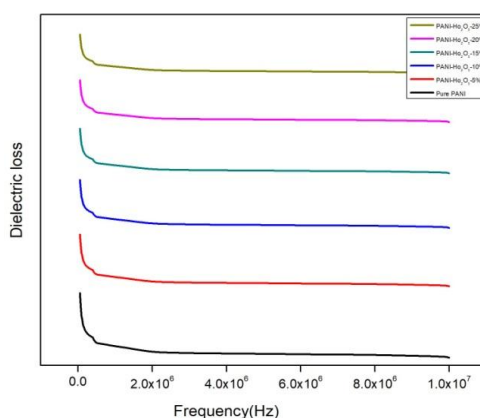
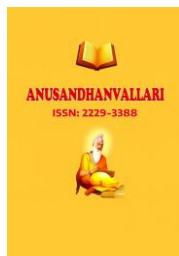


**Figure 12: Dielectric loss of Pure PANI and PANI-Ho<sub>2</sub>O<sub>3</sub> Composites**



#### 4. Conclusion:

The characterization of pure PANI and holmium oxide ( $\text{Ho}_2\text{O}_3$ )doped PANI synthesized with ammonium dichromate (ADC) leads to the following conclusions. XRD analysis confirms the formation of a hybrid system where crystalline holmium oxide nanoparticles (average crystallite is 20 nm) are successfully embedded within the semi-crystalline PANI matrix. FTIR spectroscopy verifies the emeraldine salt state of PANI and highlights strong interfacial interactions, likely through hydrogen bonding, between the polymer amino groups and the  $\text{Ho}_2\text{O}_3$  surface. FESEM analysis confirms that  $\text{Ho}_2\text{O}_3$  nanoparticles are successfully encapsulated within the globular PANI matrix, creating an interconnected network for charge transport. Both AC conductivity and DC conductivity peak at 25% wt% loading, demonstrating that holmium oxide significantly enhances the hopping of charge carriers (polarons) through the polymer. The dielectric constant and dielectric loss increase with filler concentration due to Maxwell-Wagner-Sillars (MWS) interfacial polarization, showing high stability across a wide frequency range. The nanocomposites exhibit superior thermal robustness compared to pure PANI, maintaining stable electrical properties up to 200°C. The 25%  $\text{Ho}_2\text{O}_3$  composite optimized with ADC oxidant is the most effective formulation, offering a synergistic blend of high conductivity, energy storage capability, Supercapacitors, Electromagnetic Interference (EMI) Shielding, Temperature-Stable Sensor and thermal stability for advanced electronic applications.

#### 5. Reference:

- [1] Rodrigues, M. A., and De Paoli, M. A: (1991): Synthesis of polyaniline using different oxidants. Journal of Polymer Science.
- [2] Li, Z., and Gong, L. (2020): Research Progress on Applications of Polyaniline (PANI) for Electrochemical Energy Storage and Conversion.
- [3] Zhu, J., Shao, X., Li, Z., Lin, C., Wang, C., Jiao, K., Xu, J., Pan, H., and Wu, Y. (2022). Synthesis of Holmium-Oxide Nanoparticles for Near-Infrared Imaging and Dye-Photodegradation.
- [4] Banerjee S, Sarmah S, Kumar A (2009) Photoluminescence studies in HCl-doped polyaniline nanofibers.
- [5] Chuang FY, Yang SM (2008) Cerium dioxide/polyaniline core-shell nanocomposites. J Colloid Interface Sci.
- [6] Zihang Huang, Shaoxu Wang, Hui Li, Zhicheng Tan (2012) Thermal Stability of Several Polyaniline/rare earth Oxide Composites III: Polyaniline/ $\text{Nd}_2\text{O}_3$  Composites :.
- [7] Zihang Huang, Shaoxu Wang, Hui Li, Shihui Zhang, Zhicheng Tan: (2013) Thermal Stability of Several Polyaniline/rare earth Oxide: Polyaniline/ $\text{La}_2\text{O}_3$  and Polyaniline/ $\text{Sm}_2\text{O}_3$  Composites :
- [8] Wei. Y, Jang. G. W, Hsueh. K. H, MacDiarmid. A. G and Epstein. A. J: (1992). Polymer,
- [9] Zihang Huang, Shaoxu Wang, Hui Li, Zhicheng Tan (2012) Thermal Stability of Several Polyaniline/rare earth Oxide Composites III: Polyaniline/ $\text{Nd}_2\text{O}_3$  Composites: .
- [10] Rafiqi. F. A, Majid. K, Chem. Paper :2015:1331,69
- [11] Rahmankhan. M. M, Wee. Y. K, Ahmed. S. U, Naher. M, Youns. M, Mahmood. M. A. K, Int, J. Chem, React. Eng 16,1:2017.
- [12] Wang SX, Sun LX, Tan ZC, Xu E, Li Ys, Zhang T, J Therm and Anal Calorim (2007) Synthesis, characterization and thermal analysis of polyaniline/ $\text{CO}_3\text{O}_4$  composites
- [13] Mohammad Mizanur Rahmankhan, Nurfarahhana Binti Daud, Mohammad Shahadat Hussain Chowdhury, Wan Ahmad Kamil Mahmood, Hisatoshi Kobayashi: (2013) Fabrication of polyaniline- $\text{La}_2\text{O}_3$  composite Nanofibers showing Effecting Control of Morphology, Electrical Conductivity, and Thermal Stability



- 
- [14] Manjunatha. S, Sunilkumar. A, Ravikiran. Y. T, Machappa.T: Effect of holmium oxide on impedance and dielectric behaviour of polyaniline–holmium oxide composites: 2019.
- [15] Anil Kumar, Amit Kumar, Harish Mudila, Kamendra Awasthi, Vinod Kumar:( 2020)
- [16] Synthesis and Thermal analysis of polyaniline (PANI)
- [17] Ramesan.M. T, Sampreeth. T: (2017) In situ synthesis of polyaniline/Sm-doped TiO<sub>2</sub> nanocomposites: evaluation of structural, morphological, conductivity studies and gas sensing applications
- [18] Sangshetty Kalyane: (2013) AC Conductivity Study of Polyaniline / Dysprosium Oxide (PANI / Dy<sub>2</sub>O<sub>3</sub>) Composites:
- [19] Muhammad Faisal and Syed khasim: (2019) Electrical Conductivity, Dielectric Behavior and EMI Shielding Effectiveness of Polyaniline-Yttrium Oxide Composites:.
- [20] Howell BA, Carter KE. (2012) Thermal stability of phosphinated diethyl tartrate. J Therm Anal Calorim. .
- [21] S. Manjunath, T. Machappa, A. Sunilkumar. Y.T, Ravikiran, J. Mater. Sci. 29, 1158(2018).